Dyes and Pigments 95 (2012) 126–133

Contents lists available at SciVerse ScienceDirect

Dyes and Pigments

journal homepage: www.elsevier.com/locate/dyepig

Structure–properties relationships in conjugated molecules based on diketopyrrolopyrrole for organic photovoltaics

Emilie Ripaud [a], Dora Demeter [a], Théodulf Rousseau [a], Emmanuel Boucard-Cétol [a], Magali Allain [a], Riccardo Po [b], Philippe Leriche [a,*], Jean Roncali [a,*]

[a] Group Linear Conjugated Systems, CNRS Moltech-Anjou, University of Angers, 2Bd Lavoisier, 49045 Angers, France
[b] Centro ricerche per le energie non convenzionali, Istituto ENI Donegani, ENI S.p.A.,via G. Fauser 4, 28100 Novara, Italy

ARTICLE INFO

Article history:
Received 24 November 2011
Received in revised form
16 March 2012
Accepted 19 March 2012
Available online 4 April 2012

Keywords:
Diketopyrrolopyrrole
Organic solar cell
Organic electronics
Thiophene
Furan
Structure–properties relationships

ABSTRACT

Conjugated systems built by connecting two electron-donor side-chains to a diketopyrrolopyrrole (DPP) core have been synthesized and evaluated as donor material in heterojunction organic solar cells. The effects of composition of the side-chain on the electronic properties of the conjugated system have been analyzed on first series of compounds containing various combinations of benzofuran, benzothiophene, thiophene and furan units. In a second series of compounds, the keto groups of DPP have been replaced by one or two thioketo groups. Results of UV–vis absorption spectroscopy, fluorescence emission spectroscopy and cyclic voltammetry show that the composition of the side-chain has little effect on the HOMO and LUMO levels of the system, but strongly affects the sensitivity of the material toward thermal treatment and thus indirectly the performances of the resulting solar cells. On the other hand, replacement of the keto groups of DPP by thioketo ones leads at the same time to significant reduction of the band gap due to a decrease of the LUMO level, to a quenching of fluorescence and to dramatic decrease of the photovoltaic activity of the molecule.

1. Introduction

The possibility to develop low-cost, large-area photovoltaic devices by means of low environmental impact technology has generated a considerable current interest for organic solar cells (OSCs) [1–23]. During the past decade, a multidisciplinary research effort has generated remarkable progress and power conversion efficiencies (*PCE*) in the range of 6–8% have been reported for solution-processed bulk heterojunction (BHJ) solar cells combining fullerene derivatives as acceptor material and π-conjugated polymers as donor [5–8].

In spite of these performances, the variability of the molecular weight and chain length distribution inherent to polydisperse polymers results in batch-to-batch variations that represent a possible source of problems for the reproducibility of the synthesis and purification of the material and of the performances of the resulting devices making quite difficult the analysis of structure–properties relationships. An emerging alternative or complementary approach involves the use of small molecules as donor material in solution-processed BHJ cells [9]. Molecular donors combine the advantage of unequivocal and reproducible chemical structure thus allowing a more straightforward analysis of structure–properties relationships [10]. In the past few years this approach has generated much synthetic work and many new classes of molecular donors have been synthesized and evaluated [9–23]. This effort has generated rapid progress and molecular BHJ with *PCE* in the range of 4.0–5.0% have been reported recently [21–23].

In this context, diketopyrrolopyrrole (DPP) has been a focus of particular attention as building block for the design of various classes of molecular or polymeric conjugated systems [10,14,21,24–35]. In particular, a *PCE* of 4.40% has been reported for a solution-processed BHJ combining a DPP-based donor molecule (**BFT**, Chart) and $PC_{71}BM$ as acceptor [21].

We now report on a series of DPP-based systems designed as donor material for OSCs. Two kinds of structural variations have been considered. The effects of the side-chain composition has been analyzed on **BFT**, **BTT**, **BFF** and **BTF** while the effects of the modification of the DPP core has been investigated by replacing the two keto groups of DPP by one (**BFT-OS**) and two (**BFT-SS**) thioketo groups.

The synthesis of the new compounds is described and the effects of structural variations on the electronic properties of the chromophores are discussed in relation with preliminary results on the performances of the resulting OSCs.

* Corresponding authors.
E-mail address: philippe.leriche@univ-angers.fr (P. Leriche).

0143-7208/$ – see front matter © 2012 Elsevier Ltd. All rights reserved.
doi:10.1016/j.dyepig.2012.03.021

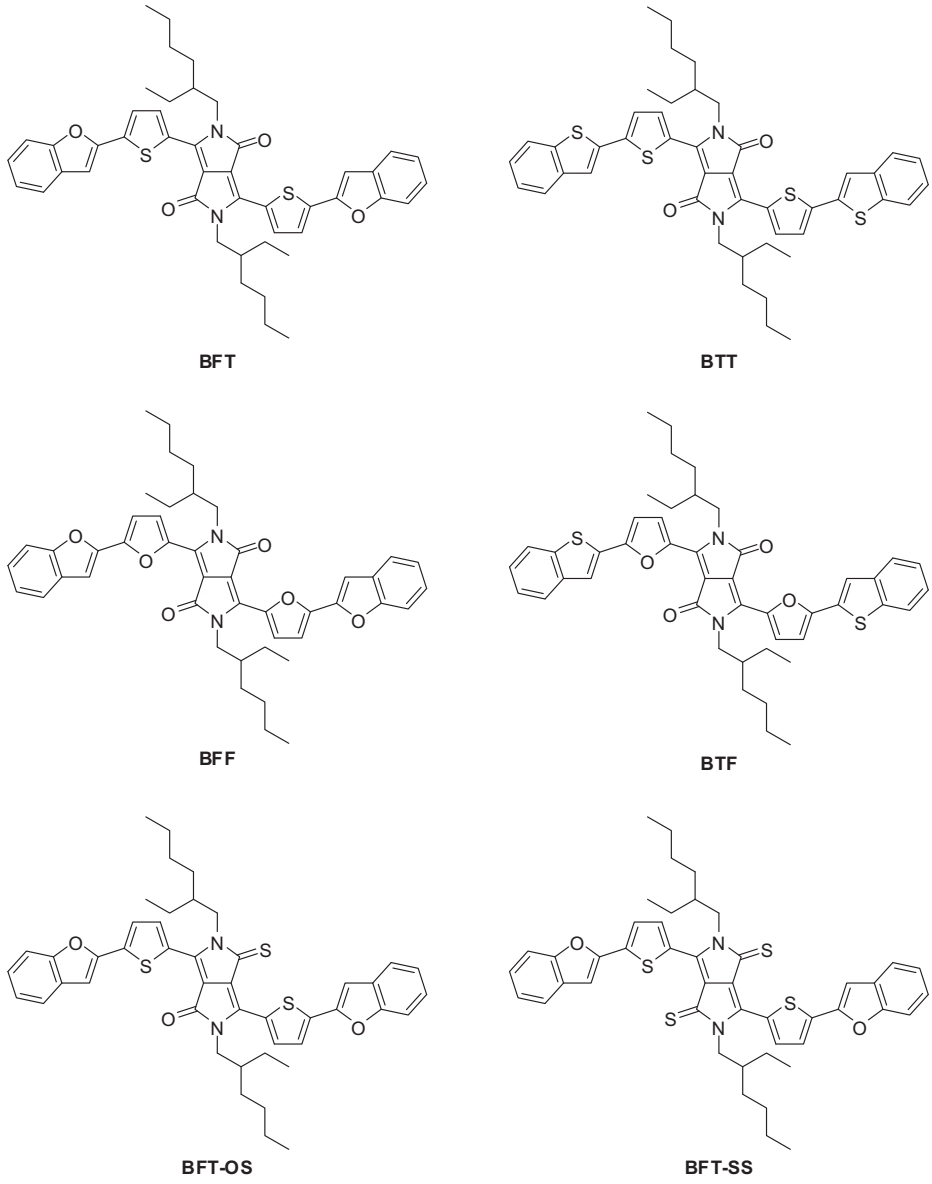

Chart.

2. Experimental

2.1. General

Solvents were purified and dried using standard protocols. ^{1}H NMR and ^{13}C NMR spectra were recorded on a Bruker AVANCE DRX 500 spectrometer operating at 300.1 and 75.4 MHz; δ are given in ppm (relative to TMS) and coupling constants (J) in Hz. Matrix-assisted laser desorption ionization time-of-flight (MALDI-TOF) mass spectra were recorded by a Bruker Biflex-III, equipped with a N_2 laser (337 nm). For the matrix, dithranol in CH_2Cl_2 was used. High resolution mass spectra were recorded under FAB mode on a Jeol JMS 700 spectrometer. UV–visible optical data were recorded with a Perkin–Elmer lambda 19 spectrophotometer. Thermal analyses were performed using a DSC 2010 CE (TA Instruments). X-ray diffraction experiments were carried out working in θ–2θ reflection mode using a Bruker D500 diffractometer equipped with a speed detector Vantec. For cyclic voltammetry (scan rate 100 mV cm^{-1}), the electrochemical apparatus consisted of a potentiostat EG&G PAR 273A and of a standard three-electrode cell. As the working and counter electrodes, a platinum foil and a platinum wire were used, respectively, while as a reference an SCE electrode served as reference.

2.2. Devices preparation and characterization

Fullerene C60 (99+%) was purchased from MER and used as received. The Baytron suspension used to apply smoothing and hole conducting/injecting layers was “Clevios P VP AI 4083” (HC Stark). All thin film devices were prepared in laboratory conditions. As electrodes, ITO coated glasses (10 Ohm/□, Kintec company) and evaporated Al films (ca. 60 nm thick) were used. The ITO electrodes were cleaned in ultrasonic baths and then modified by a spun-cast layer of Baytron (40 nm thick), which was dried at 130 °C for 15 min. The Baytron suspension was stirred and filtered through a 0.45 μm membrane (Minisart RC 15, Sartorius) just prior to casting. A 100 nm thick layer of Al was thermally evaporated

through a shadow mask, at a pressure of about 10^{-6} mbar. The mask geometry defined a device's area of 0.28 cm^2. Each ITO coated-glass substrate supported two individual devices and for each experiment a minimum of 4 devices (8 cells) was fabricated. After preparation, the devices were stored and characterized in an argon glovebox (200B, MBraun). The *J–V* curves of the devices were recorded in the dark and under illumination using a Keithley 236 source-measure unit and a homemade acquisition program. The light source was an AM 1.5 Solar Constant 575 PV simulator (Steuernagel Lichttecknik, equipped with a metal halogenide lamp). The light intensity was measured by a broad-band power meter (13PEM001, Melles Griot). The devices were illuminated through the ITO electrode side. The efficiency values reported here are not corrected, neither for the possible solar simulator spectral mismatch nor for the reflection/absorbance of the glass/ITO/Baytron coated electrodes.

2.3. Synthesis

Compounds **2**, **6** and **BFT** were synthesized as reported in the literature [21].

*3,6-Difuran-2-yl-2,5-dihydro-pyrrolo[3,4-c]pyrrole-1,4-dione (**1**)*

Under inert atmosphere, 4.5 8.26 g of sodium [0.36 mol] and a spatula tip of $FeCl_3$ are added in 2-methylbutan-2-ol (90 mL). The mixture is heated at 130 °C for 1 h. Then, 0.16 furan-2-carbonitrile (14.9 g, 0.16 mol) and 1 eq of di-tertio-amylsuccinate, (24.7 g) are introduced with an automated syringe (3 hours-10 mL/h). The mixture is stirred 3 h at 130° C. the compound is precipitated by adding an ice/methanol 3/1 (200 mL) mixture, filtered and washed with methanol to give 10.9 g (51%) of **1**. ^{1}H NMR (DMSO-d_6, ppm): 11.13 (s, 2H); 8.02 (sel, 2H); 7.65 (sel, 2H); 6.82 (sel, 2H). ^{13}C NMR (DMSO-d_6, ppm): 161.6; 146.5; 144.1; 131.8; 116.3; 113.5; 107.9. IR (cm^{-1}): 1645 (C═O); 3112 −N−H; MS (MALDI-TOF, M+•): calcd :268.05, found: 268.50.

*2,5-Bis-(2-ethyl-hexyl)-3,6-difuran-2-ylpyrrolo[3,4-c]pyrrole-1,4-dione (**3**)*

Under inert atmosphere, 3,6-difuran-2-yl-2,5-dihydro-pyrrolo [3,4-c] pyrrole-1,4-dione 1 (10.8 g, 0.04 mol) 5 eq of 1-bromo-2-ethylhexane and 4 eq of K_2CO_3 are suspended in 25 mL of dry DMF. The mixture is heated at 130 °C and the reaction is monitored by TLC. After cooling to rt, 400 mL of dichloromethane are added. The organic phase is washed with water and dried over $MgSO_4$. After removal of the solvent, the residue is chromatographed on silica gel (DCM/PE: 2/1) to give 13 g (66%) of **3**. ^{1}H NMR ($CDCl_3$, ppm): 8.33 (d, 2H, 3*J* = 3.6 Hz); 7.61 (d, 2H, 3*J* = 1.8 Hz); 6.69 (dd, 2H, 3*J* = 1.8 Hz, 3*J* = 3.6 Hz); 4.06 (m, 4H); 1.5–1.6 (m, 2H); 1.2–1.4 (m, 16H); 0.8–1.0 (m, 12H); IR (cm^{-1}); 1659 (C═O); 2856–2925–2957 (alkyl chains); 3112 (N−H); HRMS (M+•): calcd 492.2983, found 492.2978.

*2,5-Bis-(2-ethyl-hexyl)-3,6-di(2-bromofurane)-5-ylpyrrolo[3,4-c] pyrrole-1,4-dione (**5**)*

In the dark, at 0 °C, 2.2 eq of NBS are added to 2,5-bis-(2-ethylhexyl)-3,6-difuran ylpyrrolo-2-[3,4-c] pyrrole-1,4-dione 3 (12.6 g, 25.6 mmol) in 100 mL of chloroform. The mixture is stirred under inert atmosphere at rt 15 h. The reaction mixture is washed with water 3 × 300 mL, the organic phase is dried over $MgSO_4$ and filtered. After evaporation of the solvent, the residue is precipitated with hexane to give 9 g (54% yield) of a violet powder. ^{1}H NMR ($CDCl_3$, ppm): 8.30 (d, 2H, 3*J* = 3.6 Hz); 6.62 (d, 2H, 3*J* = 3.6 Hz); 3.99 (m, 4H); 1.5–1.6 (m, 2H); 1.2–1.4 (m, 16H); 0.8–1.0 (m, 12H). ^{13}C NMR ($CDCl_3$, ppm): 160.9; 146.2; 132.8; 126.3; 122.2; 115.5; 106.3; 46.3; 40.1; 30.5; 28.7; 23.8; 23.2; 14.1; 10.7. MS (MALDI-TOF, M+•): calcd 650.12, found 682.10.

*2,5-Bis(2-ethyl-hexyl)-3,6-bis(5-(benzofuran-2-yl)furan-2-yl) pyrrolo[3,4-c]pyrrole-1,4-dione (**BFF**)*

In a Schlenk under inert atmosphere, to a solution of **5** (0.2 g, 0.307 mmol) in 20 mL of toluene degassed with argon are added successively 2.2 eq of 2-trimethylstannylbenzo[*b*]thiophene and 0.2 eq of $Pd(PPh_3)_4$. The mixture is heated 15 h at 120 °C under inert atmosphere. After removal of toluene and dissolution in CH_2Cl_2 the target compound is precipitated with hexane to give 0.267 (75%) of a blue-violet product. ^{1}H NMR ($CDCl_3$, ppm): 8.5 (d, 2H, 3*J* = 3.8 Hz); 7.6 (d, 2H, 3*J* = 7.5 Hz); 7.5 (d, 2H, 3*J* = 7.5 Hz); 7.3 (m, 4H); 7.06 (d, 2H, 3*J* = 4 Hz); 7.05 (s. 2H); 4.15 (d. 4H, 3*J* = 7.6 Hz); 1.5–1.6 (m, 2H); 1.2–1.4 (m, 16H); 1.0–0.8 (m, 12H). ^{13}C NMR ($CDCl_3$, ppm): 161.0; 155.1; 148.3; 146.6; 144.7; 132.7; 128.3; 125.5; 123.58; 122.4; 121.4; 111.3; 111.3; 107.6; 103.8; 46.7; 39.6; 30.3; 28.5; 23.5; 23.2; 14.1; 10.5. HRMS (M+•): calcd 724.3507, found 724.3497.

*2,5-Bis(2-ethyl-hexyl)-3,6-bis(5-(benzothiophen-2-yl)furan-2-yl) pyrrolo[3,4-c]pyrrole-1,4-dione (**BTF**)*

In a Schlenk under inert atmosphere, to a solution of **5** (0.2 g, 0.307 mmol) in 20 mL of toluene degassed with argon are added successively 2.2 eq of 2-trimethylstannylbenzo[*b*]thiophene and 0.2 eq of $Pd(PPh_3)_4$. The mixture is heated 15 h at 120 °C under inert atmosphere. After removal of toluene and dissolution in CH_2Cl_2 the target compound is precipitated with hexane to give 0. 235 g (47%) of a blue-violet product. ^{1}H NMR ($CDCl_3$, ppm): 8.48 (d, 2H, 3*J* = 3.8 Hz); 7.8 (m, 4H); 7.56 (s, 2H); 7.35 (m, 4H); 6.90 (d, 2H, 3*J* = 3.8 Hz); 4.12 (d, 4H, 3*J* = 7.6 Hz); 1.5–1.6 (m, 2H); 1.2–1.4 (m, 16H); 0.8–1.0 (m, 12H). ^{13}C NMR ($CDCl_3$, ppm): 161.2; 152.0; 144.4; 140.0; 132.8; 131.7; 131.0; 128.9; 125.4; 125.1; 124.1; 122.9; 122.4; 121.0; 110.9; 46.8; 39.5; 30.4; 28.6; 23.5; 23.3; 14.1; 10.6. HRMS (M+•): calcd 756.3055, found 756.3029.

*2,5-Bis(2-ethyl-hexyl)-3,6-bis(5-(benzothiophen-2-yl)thiophen-2-yl)pyrrolo[3,4-c]pyrrole-1,4-dione (**BTT**)*

In a Schlenk under inert atmosphere, to a degassed toluene solution of **6** (0.2 g, 0.29 mmol) are added 2.2 eq of 2-trimethylstannylbenzo[*b*]thiophene and 0.2 eq of $Pd(PPh_3)_4$ were. The mixture is heated 15 h at 120 °C. After evaporation of toluene and dissolution in methylenechloride the product is precipitated with hexane. Chromatography on neutral alumina (DCM/Hex: 2/1) gave 48% of the target compound. ^{1}H NMR ($CDCl_3$, ppm): 8.96 (d, 2H, 3*J* = 4 Hz); 7.79 (m, 4H); 7.55 (s, 2H); 7.43 (d, 2H, 3*J* = 4 Hz); 7.36 (m, 4H); 4.07 (dd, 4H, 3*J* = 3.3 Hz, 3*J* = 7.7 Hz); 1.50–1.60 (m, 2H); 1.20–1.40 (m, 16H); 0.80–1.0 (m, 12H); ^{13}C NMR ($CDCl_3$, ppm): 161.6; 150.8; 142.6; 140.1; 135.8; 134.4; 129.2; 125.3; 125.0; 123.9; 122.2; 121.4; 121.4; 114.7; 108.7; 46.1; 31.9; 28.6; 23.7; 23.1; 22.7; 14.1; 10.6; HRMS (M+•): calcd 811.2491, found 811.2492.

*2,5-Diethylhexyl-3,6-bis(5-(benzofuran-2-yl)thiophen-2-yl)-pyrrolo[3,4-c]pyrrole-1,4-dithione (**BFT-SS**)*

A mixture of **BFT** (100 mg, 0.13 mmol) and Lawesson's reagent (220 mg, 0.53 mmol), in 30 mL of anhydrous toluene is refluxed overnight under argon. After concentration, the residue is chomatographed on silica gel (eluent dichloromethane/petroleum ether: 2/1) to give to a black solid, which is recrystallized from ethanol (50 mg, yield = 50%). M.p. 201–202 °C. ^{1}H NMR (300 MHz, $CDCl_3$): 8.96 (d, 2H, *J* = 4.0 Hz); 7.62–7.51 (m, 6H); 7.37–7.24 (m, 4H), 7.09 (s, 2H), 4.59–4.57 (m, 4H), 1.86–1.82 (m, 2H), 1.25–1.19 (m, 16H), 0.82–0.77 (m, 12H). ^{13}C NMR (300 MHz, $CDCl_3$): 176.7, 155.0, 149.9, 143.4, 139.0, 135.3, 128.8, 126.9, 125.7, 125.4, 124.5, 123.5, 121.2, 111.3, 103.8, 48.5, 38.6, 30.2, 28.4, 23.6, 22.9, 13.9, 10.7. MS MALDI:

789.0 [$M^{+\bullet}$]. HRMS *m/z*: [M^+] calcd for $C_{46}H_{48}N_2O_2S_4$: 788.2593, found 788.2593. [M^+Na]$^+$ calcd for $C_{46}H_{48}N_2O_2NaS_4$: 811.2490, found 811.2489.

*2,5-Diethylhexyl-3,6-bis(5-(benzofuran-2-yl)thiophen-2-yl)-pyrrolo[3,4-c]pyrrole-1,4-dionothione (**BFT-OS**)*

This compound was isolated from the same reaction medium (20 mg, yield 20%), and purified by silica gel chromatography using the same eluting conditions. The limited stability of this compound did not allow its proper characterization by NMR. MS MALDI: 773.0 [$M^{+\bullet}$]. HRMS *m/z*: [M^+H]$^+$ calcd for $C_{46}H_{49}N_2O_3S_3$: 773.2899, found 773.2904.

3. Results and discussion

3.1. Synthesis

The target compounds have been synthesized by condensation of a dialkylsuccinate with a cyanoaryl compound. An analysis of the reaction conditions has shown that the use of a sterically demanding branched alkyl chain leads to better results. Therefore, the diisoamyl succinate prepared in 90% yield using a known procedure [36] has been used for the synthesis of compounds **1** and **2** in 73 and 51% respectively (Scheme 1). In order to ensure the solubility of the final compounds, alkylation of the two nitrogen atoms of DPP was achieved using the appropriate bromo-alkane in the presence of cesium carbonate to give compounds **3** and **4** in 66 and 31% yield respectively. Bromination of the resulting tricyclic compounds with NBS in chloroform gave the corresponding dibromo-compounds **5** and **6** (54 and 43% yield). Coupling of compounds **5** and **6** with the Stille reagent of benzothiophene or benzofuran gave the target compounds in 50–70% yield.

The thioketo (**BFT-OS**) and dithioketo (**BFT-SS**) compounds were isolated in 20 and 50% yield by reaction of **BFT** with the Lawesson reagent in refluxing toluene. Surprisingly **BFT-OS** was obtained as oil and showed a limited stability. The targets compounds have been satisfactorily characterized by ^1H and ^{13}C NMR and mass spectrometry. However, due to its lack of stability, (**BFT-OS**) could not be fully characterized nor evaluated in OSC devices.

The thermal stability of the target compounds has been investigated by differential scanning calorimetry and thermogravimetry. All compounds with a classical DPP are thermally stable and show decomposition temperature much higher than their melting point except for the all-furan compound **BFF** which decomposes at 195 °C. The introduction of thioketo groups in the structure produces drastic changes in the thermal properties and **BFT-SS** does not melt but decomposes at 162 °C (Table 1).

3.2. Electronic properties of the donors

The electronic properties of the compounds have been analyzed by UV–vis absorption spectroscopy, fluorescence emission spectroscopy and cyclic voltammetry. The UV–vis data recorded in CH_2Cl_2 solutions show that the composition of the side-chains has little influence on the optical properties of the system. Thus, the maximum of the absorption band of lowest energy (λ_{0-0}) shows only a 12 nm red shift when replacing the all-furan chain of **BFF** (616 nm) by the mixed benzofuran-thiophene **BFT** (628 nm). On the other hand, the four compounds present high molecular absorption coefficients (ε) (Table 2).

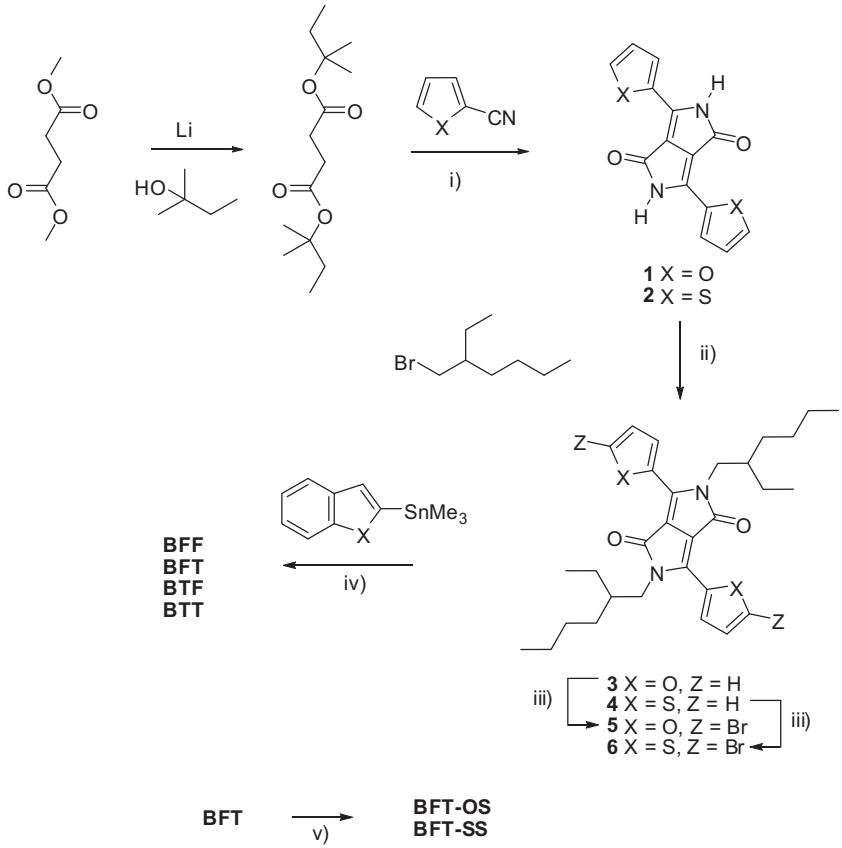

Scheme 1. Synthesis of the target compounds. i) $FeCl_3$, Na, *t*-AmOH; ii) DMF, K_2CO_3, 130 °C; iii) NBS, $CHCl_3$, rt; iv) $Pd(PPh_3)_4$, toluene; v) LR, toluene.

Table 1
Melting points and thermal decomposition temperature of the target compounds.

Compd	Mp (°C)	Td (°C)
BTF	247	347
BFF	–	195
BFT	222	280
BTT	265	327
BFT-SS	–	162

Table 2
UV–is absorption and fluorescence emission data of the compounds in CH_2Cl_2, E_g of materials in the solid states (from 1 mg mL^{-1} chloroform spin coated solutions).

Compd	λ_{max} (nm	ε (M^{-1} cm^{-1})	λ_{em} (nm)	ϕ (%)	ΔE (eV)	E_g (eV)
BTF	358, 570, 620	72,400	632–685	42	2.00	1.76
BFF	352, 566, 616	85,500	626–680	53	2.01	1.81
BFT	354, 583, 628	54,500	647–700	26	1.97	1.76
BTT	356, 584, 624	53,200	650–700	34	1.99	1.69
BFT-SO	335, 475, 688	9500	nd	nd	1.80	nd
BFT-SS	396, 503, 718	11,600	nf	–	1.73	1.55

It is known that replacement of the keto groups of DPP by thioketo ones produces a red shift of the absorption spectrum.[36] This effect is also observed here and the introduction of one and two thioketo groups in the structure produces a large bathochromic shift of λ_{0-0} to 688 and 718 nm for **BFT-OS**, and **BFT-SS** respectively accompanied by a significant decrease of ε (Fig. 1 and Table 2).

The UV–vis absorption spectra of films spun-cast on glass from chloroform solutions (see SI) reveal large bathochromic shifts of the absorption maxima with a broadening of the absorption bands while the low energy absorption edges lead to optical band gaps (E_g) in the range of 1.70–1.80 eV. Comparison of the E_g values shows that the increase of the thiophene content leads to a small reduction of E_g from 1.81 eV for **BFF** to 1.69 eV for **BTT**. On the other hand, replacement of the carbonyl groups by thiocarbonyl ones produces a more drastic effect with a reduction of E_g down to 1.55 eV for **BFT-SS** (Table 2).

The fluorescence emission properties have been measured in CH_2Cl_2 solution using cresyl violet in ethanol as standard (ϕ_{em} = 0.54). All compounds with a classical DPP system show fluorescence quantum yields in the range of 35–50%, the highest values being observed for compounds with a furan ring directly connected to the DPP core **BTF** and **BFF**. A most striking phenomenon is that replacement of the carbonyl groups by thiocarbonyl ones in **BFT-SS** results in a complete quenching of fluorescence.

Fig. 2 shows the cyclic voltammograms corresponding to the oxidation and reduction of **BFT**, **BFT-OS** and **BFT-SS** in the presence of tetrabutylammonium hexafluorophosphate in CH_2Cl_2. The four compounds containing diketo-groups present a very similar CV response with two reversible one-electron oxidation processes with anodic peak potentials $E_{pa}1$ and $E_{pa}2$ around 0.70–0.80 and 1.00 V (Table 3).

The CV of **BTF** and **BFF**, with a furan ring adjacent to the DPP core presents slightly less positive $E_{pa}1$ values. This difference could reflect a better π-electron delocalization associated with the lower resonance energy of furan compared to thiophene. However the smaller dihedral angle between the DPP core and the linked furan ring could also play a role. This hypothesis is consistent with crystallographic and theoretical results (see SI). As shown in Fig. 2, all compounds are reversibly reduced with cathodic pic E_{pc} around −1.10 V for compounds with a diketo core. The introduction of thioketo groups produces a positive shift of E_{pc} to −0.90 and −0.80 V for **BFT-OS** and **BFT-SS** respectively indicating a decrease of the LUMO energy level (Table 3).

As shown by these optical and electrochemical results, the composition of the side-chain has little influence on the energy level of the frontier orbitals of the molecule and hence on the band gap of the resulting material. On the other hand, the introduction of

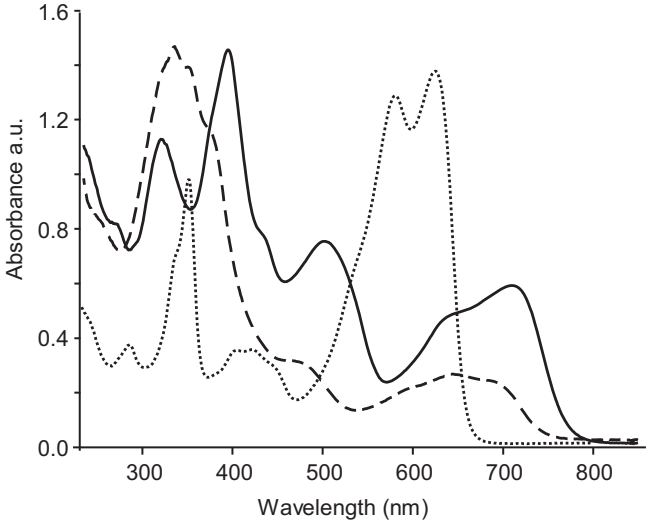

Fig. 1. UV–vis absorption spectra of **BFT** (dotted line), **BFT-OS** (dashed line) and **BFT-SS** (solid line) in dichloromethane.

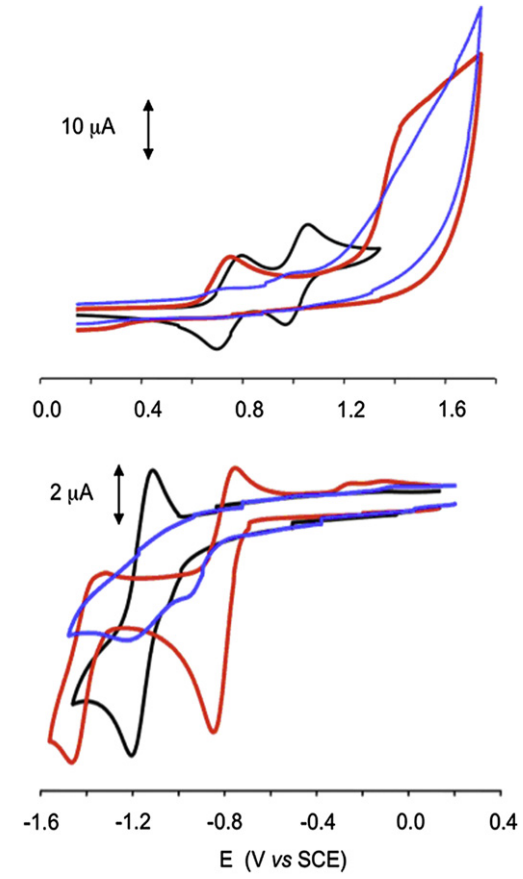

Fig. 2. Cyclic voltammograms of **BFT** (black), **BFT-OS** (blue) and **BFT-SS** (red). Top: oxidation in 0.10 M Bu_4NPF_6/CH_2Cl_2, bottom: reduction in 0.10 M Bu_4NPF_6/THF, scan rate 100 mV s^{-1}. (For interpretation of the references to colour in this figure legend, the reader is referred to the web version of this article.)

Table 3
Cyclic voltammetric data for the donors recorded in the conditions of Fig. 2.

Compd	$E_{pa}1$ (V)	$E_{pa}2$ (V)	E_{pc} (V)	E_{HOMO}[a] (eV)	E_{LUMO} (eV)
BTF	0.71	0.98	−1.06	−5.65	−3.88
BFF	0.75	1.01	−1.08	−5.69	−3.86
BFT	0.77	1.04	−1.09	−5.71	−3.85
BTT	0.81	1.04	−1.08	−5.75	−3.86
BFT-SO	0.72	0.98	−0.90	−5.66	−4.04
BFT-SS	0.74	1.44	−0.80	−5.68	−4.14

[a] Assuming $E_{ENH} = -4.6$ eV.

thioketo groups in the structure produces a significant reduction of E_g due to and a *ca* 0.30 eV decrease of the LUMO level together with a decrease of the absorption coefficient and complete quenching of fluorescence.

3.3. Evaluation of the donors in organic solar cells

The potentialities of the various compounds as donor material in heterojunction OSCs have been evaluated on bilayer devices using vacuum deposited C_{60} as acceptor layer. Although bulk heterojunction lead in general to better *PCE*, bilayer cells appear more reliable for screening experiments on new compounds available only in limited amounts. The cells were fabricated by spin-casting a film of donor of typically 20 nm on an ITO electrode pre-coated with a 40 nm film of PEDOT-PSS. A 50 nm layer of C_{60} was then thermally evaporated under vacuum and the device was completed by a 100 nm thick layer of aluminum electrode.

Fig. 3 shows the incident photon to electron conversion efficiencies (*IPCE*) spectra of the cells based on the donors with diketo-DPP core before and after thermal annealing. Indeed, numerous studies have shown that thermal treatment may strongly affect the morphology of the active layer with an increase of the crystallinity of the materials propitious to an increased optical density and charge mobility and thus to a better Jsc. IPCE spectra show that despite their comparable electronic properties the four donors lead to considerably different photoresponses. The all-thiophene **BTT** leads to the lowest peak intensity. After annealing, the highest *IPCE* is obtained with **BFT** with a 38% peak at 600 nm. The all-furan **BFF** derivative which presented the higher IPCE before annealing only shows a moderate improvement from 10 to 15% as **BTF** doesn't exhibit a real improvement at 12%. It is noteworthy that intensity of the *IPCE* response is tightly correlated with the sensitivity toward thermal treatment. Thus, the largest difference between the spectra recorded before and after thermal annealing is observed for **BFT** which is the most efficient donor while in contrast, thermal treatment has no effect on the photoresponse of the poorly efficient **BTT** cell; we note only a decrease of the absorbance of beyond 200 °C. On the other hand, the lack of improvement observed after thermal treatment of **BFF** is mainly due to its thermal instability. In fact, contrary to **BFT**, **BFF** does not present a clear melting point but a thermal decomposition at 195 °C.

The current *vs* voltage curves of the various cells have been recorded under simulated solar irradiation in AM 1.5 conditions with a power light intensity of 90 mW cm^{-2}. The data in Table 4 confirm, in agreement with the *IPCE* spectra, that **BFT** leads to the highest efficiency, with a short-circuit current density (J_{sc}) close to 8.0 mA cm^{-2} and a *PCE* of 2.50% (Fig. 4). As expected **BTT** leads to low J_{sc} and *PCE* while **BFF** and **BTF** gave values around 0.80% with J_{sc} values of ~3.0 mA cm^{-2}.

The results also confirm the already observed strong dependence of the cell performances on the sensitivity toward thermal treatment with the largest effect observed with **BFT** and no effect for **BTT**. Finally we note that no significant photovoltaic effect could be observed for the cells based on **BFT-SS** which gave only negligible currents.

In order to complete these observations, **BFT-SS**, was also evaluated in BHJ cells using **BFT** as a reference. The devices were realized with $PC_{61}BM$ as acceptor using a 3:2 donor/acceptor weight ratio in chloroform. Fig. 5 shows the *J vs V* curves obtained under white light illumination. Again a considerable effect of thermal annealing is observed for **BFT** with an increase of J_{sc} from

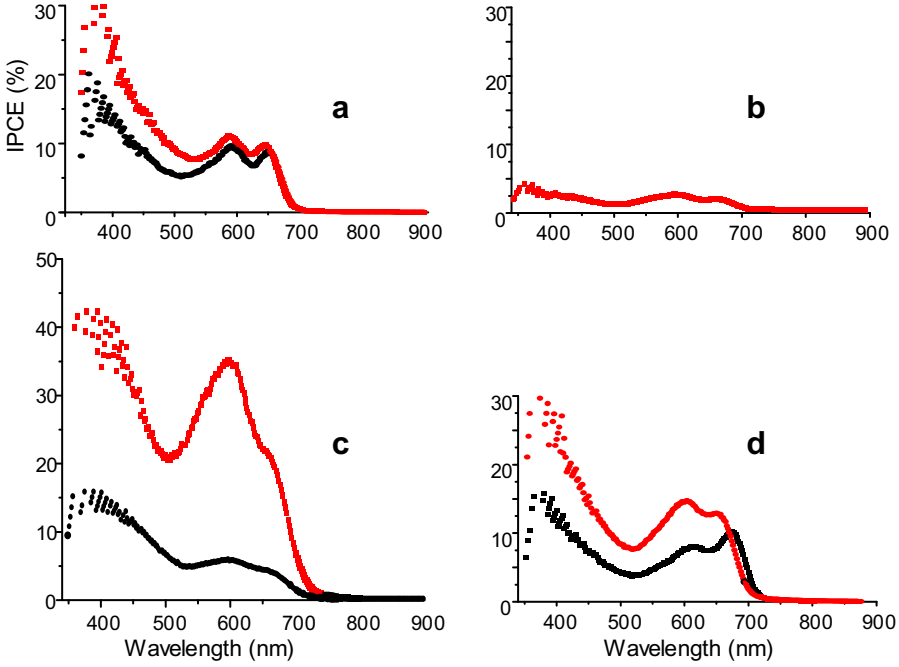

Fig. 3. *IPCE* spectra of bilayer solar cells based on DPP donors and C_{60}. (a) **BTF**, (b) **BTT**, (c) **BFT**, (d) **BFF**. Black line: as cast films, red line after 10 min thermal treatment. **BFT** 130 °C, **BTT** no thermal treatment, **BTF** 90 °C, **BFF**, 120 °C. (For interpretation of the references to colour in this figure legend, the reader is referred to the web version of this article.)

Table 4
Photovoltaic parameters of bilayers solar cells based on DPP donors and C_{60}. Under white light illumination at 90 mW cm^{-2}. Data in bold have been measured after thermal annealing in the conditions of Fig. 3.

Compd	J_{sc} (mA cm^{-2})	V_{oc} (V)	*FF* (%)	*PCE* (%)
BTF	1.80	0.67	24	0.33
	3.22	**0.66**	**32**	**0.75**
BTT	0.13	0.39	19	0.01
BFT	2.50	0.61	41	0.70
	7.90	**0.72**	**39**	**2.50**
BFF	1.60	0.51	28	0.30
	3.30	**0.60**	**39**	**0.80**
BFT-SS	0.003	0.09	25	<0.001

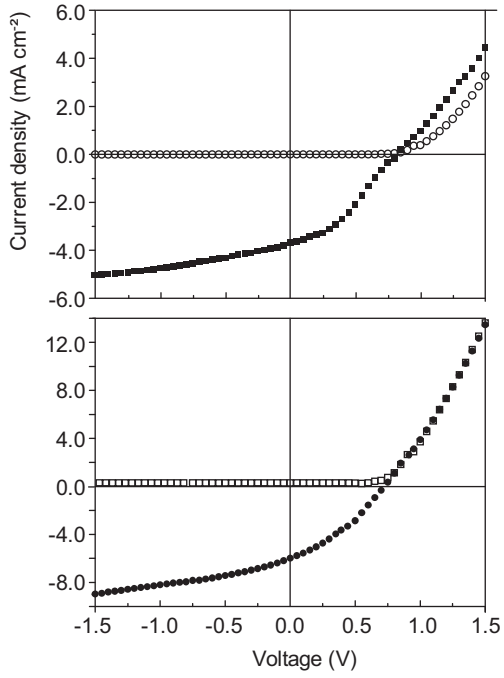

Fig. 4. Current density *vs* voltage curves of bilayer solar cells donor/C_{60}, (after thermal treatment in the conditions of Fig. 3), in the dark (empty squares) and under simulated solar irradiation in AM 1.5 conditions at 90 mW cm^{-2}. Top: **BTF**, bottom: **BFT**.

3.30 to 10.0 mA cm^{-2} while *PCE* increases from 0.92 to 3.13%. On the other hand, the results obtained with the **BFT-SS** cells confirm the absence of photovoltaic effect of this donor (Table 5).

The *IPCE* spectra of the two types of cells agree well with the above results and confirm the large effect of thermal treatment on the **BFT** cells. The spectrum shows a first peak a *ca* 450 nm followed by a major band of 65% around 600 nm. For **BFT-SS** the major peak of 25% around 400 nm essentially reflects the contribution of $PC_{61}BM$ while a peak of less than 0.05% is observed at the maximum of the long wavelength absorption band of the donor.

These results confirm that despite a noticeable reduction of the band gap **BFT-SS** does not exhibit any photovoltaic effect when used as donor with C_{60}-based acceptors. A first explanation of this phenomenon could be related to the *ca* 0.30 eV lower LUMO level of **BFT-SS** compared to **BFT** which results in a decrease of the driving force for photo-induced electron transfer to C_{60}. On the other hand, the quenching of luminescence resulting from the introduction of thioketo groups in the structure suggests a considerable reduction of the lifetime of the singlet excited state which can also contribute to reduce the probability of photo-induced electron transfer.

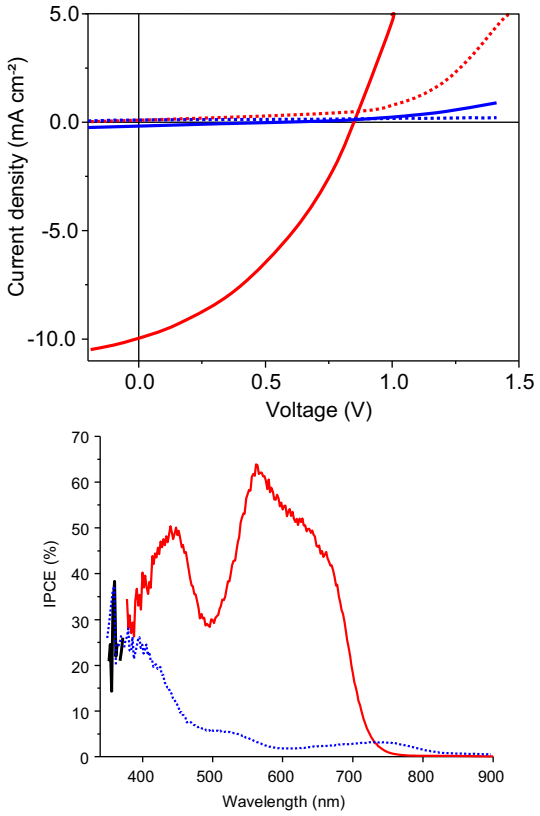

Fig. 5. Top: Current density *vs* voltage curves for BHJ solar cells based on **BFT** (red) and **BFT-SS** (blue). Bottom *IPCE* spectra of the two cells. The cells were subjected to thermal treatment (10 min at 70 °C). (For interpretation of the references to colour in this figure legend, the reader is referred to the web version of this article.)

Table 5
Photovoltaic parameters of bulk heterojunction solar cells based on based on **BFT** and **BFT-SS** and $PC_{61}BM$ under simulated solar irradiation AM 1.5 conditions, at 90 mW cm^{-2}. Results in bold are measured after thermal treatment (10 min at 70 °C).

Compd	J_{sc} (mA cm^{-2})	V_{oc} (V)	*FF* (%)	*PCE* (%)
BFT	3.30	0.94	27	0.92
	10.01	**0.81**	35	**3.13**
BFT-SS	0.008	0.46	25	<0.001
	0.007	**0.40**	**22**	**<0.001**

4. Conclusion

New DPP-based D–A–D molecules have been synthesized. Optical and electrochemical data show that the modification of the side-chain composition has little effect on the energy level of the molecule but strongly affects the efficiency of the resulting photovoltaic devices. This effect seems to be tightly correlated to sensitivity of the material toward thermal annealing. This suggests that besides appropriate light-harvesting properties and energy levels, the ability of DPP-based donors to reorganize in the solid-state is crucial for the fabrication of efficient solar cells. Replacement of the carbonyl groups of DPP by thioketo groups produces a significant reduction of the band gap of the material due essentially to the decrease of the LUMO level. However, these modifications are accompanied with a complete quenching of fluorescence and photovoltaic conversion efficiency. Although these new compounds did not allow the fabrication of highly efficient solar cells, this first step in the

analysis of structure–properties relationships of DPP-based molecular donors has provided some informations that could be useful for further work on the design of active materials for OSCs.

Acknowledgments

We thank the French Ministry of Research for the PhD grant of E.R and T.R, and ENI company for financial support.

Appendix A. Supplementary information

Supplementary data related to this article can be found online at doi:10.1016/j.dyepig.2012.03.021.

References

[1] Thompson BC, Fréchet JMJ. Polymer-fullerene composite solar cells. Angew Chem Int Ed 2008;47(5):58.
[2] Gunes S, Neugebauer H, Sariciftci NS. Conjugated polymer-based organic solar cells. Chem Rev 2007;107:1324.
[3] Dennler G, Scharber MC, Brabec CJ. Polymer-fullerene bulk-heterojunction solar cells. Adv Mater 2009;21:1323.
[4] Po R, Maggini M, Camaioni N. Polymer solar cells: recent approaches and achievements. J Phys Chem C 2010;114:695.
[5] Kim K, Liu J, Namboothiry MAG, Carroll DL. The role of donor and acceptor nanodomains in 6% thermally annealed polymer photovoltaîcs. Appl Phys Lett 2007;90: 163511.
[6] Park SH, Roy A, Beaupre S, Cho S, Coates N, Moon JS, et al. Bulk heterojunction solar cells with internal quantum efficiency approaching 100%. Nat Photon 2009;3:297.
[7] Liang LL, Xu Z, Xia JB, Tsai ST, Wu Y, Li G, et al. For the bright future-bulk heterojunction polymer solar cells with power conversion efficiency of 7.4%. Adv Mater 2010;22:E135.
[8] He Z, Zhong C, Huang X, Wong WY, Wu H, Chen L, et al. Simultaneous enhancement of open-circuit voltage, short-circuit current density, and fill factor in polymer solar cells. Adv Mater 2011;23:4636.
[9] (a) Roncali J, Frère P, Blanchard P, de Bettignies R, Turbiez M, Roquet S, et al. Molecular and supramolecular engineering of p-conjugated systems for photovoltaic conversion. Thin Solid Films 2006;511–512:567;
(b) Roquet S, de Bettignies R, Leriche P, Roncali J. Three dimensionnal tetra(oligothienyl)silanes as donors material for organic solar cells. J Mater Chem 2006;16:3040.
[10] For reviews see: (a) Lloyd MT, Anthony JE, Malliaras G. Photovoltaics from soluble small molecules. Mater Today 2007;10:34;
(b) Roncali J, Leriche P, Cravino A. From one- to three-dimensional organic semiconductors: in search of the organic silicon. Adv Mater 2007;19:2045;
(c) Roncali J. Molecular bulk heterojunction: an emerging approach to organic solar cells. Acc Chem Res 2009;42:1719;
(d) Tang W, Hai J, Dai Y, Huang Z, Lu B, Yuan F, et al. Recent development of conjugated oligomers for high-efficiency bulk-heterojunction solar cells. Solar Energy Mater Solar Cells 2010;94:1963;
(e) Walker B, Kim C, Nguyen TQ. Small molecule solution-processed bulk heterojunction solar cells. Chem Mater 2011;23:470.
[11] Roquet S, Cravino A, Leriche P, Alévêque O, Frère P, Roncali J. Hybrid systems with internal charge transfer as donor materials for heterojunction solar cells. J Am Chem Soc 2006;128:3459.
[12] Valentini L, Bagnis D, Marrochi A, Seri M, Taticchi A, Kenny JM. Novel anthracene-core molecule for the development of efficient PCBM-based solar cells. Chem Mater 2008;20:32.
[13] Lincker F, Delbosc N, Bailly S, De Bettigines R, Billon M, Pron A, et al. Fluorenone-based molecules for bulk-heterojunction solar cells: synthesis, characterization, and photovoltaic properties. Adv Funct Mater 2008;18:3444.
[14] Tamayo B, Walker B, Nguyen TQ. A low band gap, solution processable oligothiophene with a diketopyrrolopyrrole core for use in organic solar cells. J Phys Chem C 2008;112:11545.
[15] Kroneneberg NM, Deppish M, Würthner F, Ledemann HWA, Deing K, Meerholz K. Bulk heterojunction organic solar cells based on merocyanine colorants. Chem Commun; 2008:6489.
[16] Silvestri F, Irwin MD, Beverina F, Facchetti A, Pagani GA, Marks TJ. Efficient squaraine-based solution processable bulk-heterojunction solar cells. J Am Chem Soc 2008;130:17640.
[17] Rousseau T, Cravino A, Bura T, Ulrich G, Ziessel R, Roncali J. Bodipy derivatives as donor materials for bulk heterojunction solar cells. Chem Commun; 2009:1673.
[18] Zhao X, Piliego C, Kim B, Poulsen DA, Ma B, Unruh DA, et al. Solution-processable crystalline platinum-acetylide oligomers with broadband absorption for photovoltaic cells. Chem Mater 2010;22:2325.
[19] Mikroyannidis JA, Kabanakis AN, Balraju P, Sharma GD. Bulk heterojunction photovoltaics using broad absorbing small molecules based on 2-styril-5-phenylazo-pyrrole. Langmuir 2010;26:17739.
[20] Liu Y, Wan X, Yin B, Zhou J, Long G, Yin S, et al. Efficient solution processed bulk-heterojunction solar cells based a donor–acceptor oligothiophene. J Mater Chem 2010;20:2464.
[21] Walker B, Tamayo AB, Dang XD, Zalar P, Seo JH, Garcia A, et al. Nanoscale phase separation and high photovoltaic efficiency in solution-processed, small-molecule bulk heterojunction solar cells. Adv Funct Mater 2009;19: 3063.
[22] Shang H, Fan H, Liu Y, Hu W, Li Y, Zhan X. A solution-processable star-shaped molecule for high-performance organic solar cells. Adv Mater 2011;23:1554.
[23] Liu Y, Wan X, Wang F, Zhou J, Long G, Tian J, et al. Spin-coated small molecules for high performance solar cells. Adv Energy Mater 2011;1:771.
[24] Chan WK, Chen Y, Peng Z, Yu L. Rational designs of multifunctional polymers. J Am Chem Soc 1993;115:11735.
[25] Hao Z, Iqbal A. Some aspects of organic pigments. Chem Soc Rev 1997;26:203.
[26] Langhals H, Potrawa T, Nöth H, Linti G. The influence of packing effect on the solid state fluorescence of diketopyrrolopyrroles. Angew Chem Int Ed Engl 1989;28:478.
[27] Beyerlein T, Tieke B. New photoluminescent conjugated polymers with 1,4-dioxo-3,6-diphenylpyrrolo[3,4-c]pyrrole (DPP) and 1,4-phenylene units in the main chain. Macromol Rapid Commun 2000;21:182.
[28] Cao D, Liu Q, Zeng W, Han S, Peng J, Liu S. Synthesis and characterization of novel red-emitting alternating copolymers based on fluorene and diketo-pyrrolopyrrole derivatives. J Polym Sci A 2006;44:2395.
[29] Vala M, Weiter M, Vynuchal J, Toman P, Lunak Jr S. Comparative studies of diphenyl-diketo-pyrrolopyrrole derivatives for electroluminescence applications. J Fluores 2008;18:1181.
[30] Zhu Y, Zhang K, Tieke B. Electrochemical polymerization of bis(3,4-ethylenedioxythiophene)-substituted 1,4-diketo-3,6-diphenyl-pyrrolo[3,4-c] pyrrole (DPP) derivative. Macromol Chem Phys 2009;210:431.
[31] Wienk MM, Turbiez M, Gilot J, Janssen RAJ. Narrow-bandgap diketo-pyrrolo-pyrrole polymer solar cells: the effect of processing on the performance. Adv Mater 2008;20:2556.
[32] Huo L, Hou J, Chen HY, Zhang S, Jiang Y, Chen TL, et al. Bandgap and molecular level control of the low-bandgap polymers based on 3,6-dithiophen-2-yl-2,5-dihydropyrrolo[3,4-c]pyrrole-1,4-dione toward highly efficient polymer solar cells. Macromolecules 2009;42:6564.
[33] Zou Y, Gendron D, Badrou-Aïch R, Najari A, Tao Y, Leclerc M. A high-mobility low-bandgap poly(2,7-carbazole) derivative for photovoltaic applications. Macromolecules 2009;42:2891.
[34] Kanimozhi C, Balraju P, Sharma GD, Patil S. Synthesis of diketopyrrolopyrrole containing copolymers: a study of their optical and photovoltaic properties. J Phys Chem B 2010;114:3095.
[35] Frei U, Kirchmayr R. US Pat. 4904814, Ciba-Geigy, 27.02.1990.
[36] Closs F, Gompper R. 2,5-Diazapentalenes. Angew Chem Int Ed Engl 1987;26: 552.